

# Exocytosis of norepinephrine at axon varicosities and neuronal cell bodies in the rat brain

Zohreh Chiti and Anja G. Teschemacher

Department of Pharmacology, School of Medical Sciences, Bristol Heart Institute, University of Bristol, University Walk, Bristol, UK

**ABSTRACT** Norepinephrine secretion from central neurons was widely assumed to occur by exocytosis, but the essential characteristics of this process remained unknown. We developed an approach to study it directly by amperometry using carbon fiber microelectrodes in organotypic rat brainstem slice cultures. Noradrenergic neurons from areas A1 and A2 were fluorescently labeled by an adenoviral vector with noradrenergic-specific promoter. Quantal events, consistent with exocytotic release of norepinephrine, were registered at noradrenergic axonal varicosities as well as at cell bodies. According to their charge integrals, events were grouped into two populations. The majority (~40 fC) were compatible with full exocytotic fusion of small clear and dense core vesicles shown in previous morphometric studies. The quantal size distribution was modulated by treatment with reserpine and amitriptyline. In addition, much larger quantal events (>1 pC) occurred at predominantly axonal release sites. The time course of signals was severalfold faster than in adrenal chromaffin cells, suggesting profound differences in the release machinery between these cell types. Tetrodotoxin eliminated the majority of events, indicating that release was partially, but not entirely, action potential driven. In conclusion, central norepinephrine release has unique characteristics, distinguishing it from those of other monoaminergic cells in periphery and brain.—Chiti, Z., Teschemacher, A. G. Exocytosis of norepinephrine at axon varicosities and neuronal cell bodies in the rat brain. *FASEB J.* 21, 2540–2550 (2007)

*Key Words:* brainstem • amperometry • organotypic slice culture • viral vector • neurosecretion

NOREPINEPHRINE (NE) IN THE BRAIN is involved in the regulation of a wide variety of vital central nervous processes ranging from appetite and blood pressure control (1) to opiate addiction (2). Numerous drugs, for example antidepressants and centrally acting antihypertensive drugs, act via modulation of NE release in the brain (3).

Despite the fundamental role of NE in brain function, the mechanisms of its release are poorly understood. Although NE secretion was assumed to occur via vesicle exocytosis, this had not been directly demon-

strated and many important characteristics of central NE release, such as kinetics of quantal events, remained unknown. Furthermore, whereas multiple NE-containing vesicle populations have been described by electron microscopical (EM) studies, their roles in NE release are currently not understood (4–7). Another unresolved issue is the distribution of release sites within noradrenergic (NEergic) neurons, a key determinant of the functional impact of secreted NE. Release from varicosities will activate receptors in distant axonal target areas such as the spinal cord, hypothalamus, or cortex, while somato-dendritic release would affect predominantly the excitability of NEergic cell bodies in an autocrine fashion. There are several lines of evidence that all suggest that NE release may occur in the proximity of NEergic somata (7, 8). However, the presence of recurrent axonal collaterals in these areas precluded a conclusive proof of somato-dendritic NE release. In contrast, the molecular processes underlying catecholamine exocytosis in peripheral models, such as adrenal chromaffin cells are well established. For example, quantal as well as vesicle sizes and temporal characteristics of release have been determined (9–11). Further, intracellular  $Ca^{2+}$  dependence, vesicle pools involved in NE release, and many of the proteins mediating and modulating vesicular fusion have been characterized (12, 13). Although neuroendocrine cells and central NEergic neurons are likely to share many mechanistic features of their transmitter release apparatus, the obvious dissimilarities in morphology, compartmentalization, and vesicle populations between the two cell types strongly suggest profound differences in the molecular composition of exocytotic machinery, vesicular matrix, and intracellular signaling pathways (reviewed in ref. 14).

To address the questions surrounding NE release in the brain, we have employed amperometry based on carbon fiber microelectrodes (CFEs) to record quantal release events from genetically targeted NEergic green fluorescent protein (EGFP)-expressing neurons in organotypic brain slice culture (15–17). Carbon fiber amperometry provides a quantitative measure of oxidiz-

<sup>1</sup> Correspondence: Department of Pharmacology, School of Medical Sciences, University of Bristol, University Walk, Bristol BS8 1TD, UK. E-mail: anja.teschemacher@bristol.ac.uk  
doi: 10.1096/fj.06-7342com

able transmitter per release quantum and has been increasingly used over the past 2 decades, for example to characterize release of NE release in chromaffin cells, in real time (18, 19). This study establishes several key characteristics of NE release from central neurons in areas A1 and A2 and demonstrates that not only axonal varicosities but also somata can release quanta of NE.

## MATERIALS AND METHODS

### Preparation of cultures

Organotypic brainstem slice cultures were prepared as detailed previously (15). Animals were treated according to British Home Office regulations. Briefly, Wistar rat pups (p8–10) were terminally anesthetized with halothane. Brainstems were rapidly removed under sterile conditions and transferred into cold dissection saline [ $\text{Ca}^{2+}$ -free Hanks' balanced salt solution (Invitrogen, Life Technologies, Carlsbad, CA, USA), containing 25.6 mM glucose, 10 mM  $\text{MgCl}_2$ , 1 mM HEPES, 1 mM kynurenic acid, 0.005% phenol red, 100 U/ml penicillin, and 0.1 mg/ml streptomycin; 4°C, pH 7.4]. The brainstem block containing the A1 and A2 NEergic cell groups was mounted on a vibratome stage and cut into 250  $\mu\text{m}$  thick sections that were kept at 4°C for 1 h. Slices were plated onto organotypic culture membranes (Millipore, Billerica, MA, USA) in enriched Optimum-1 (Invitrogen, Life Technologies) media (15). To fluorescently label NEergic neurons, slices were exposed at the time of plating to  $\sim 5 \times 10^8$  transducing units/ml of an adenoviral vector expressing EGFP under control of the PRSx8 promoter (15, 16, 20, 21). Slices were kept at interface in a humidified 5%  $\text{CO}_2$  atmosphere at 37°C, fed with enriched Neurobasal media (Invitrogen, Life Technologies) twice a week, and used for amperometric recordings between 7 and 14 days after preparation (15). For measurements, slices were excised from the culturing membrane and transferred to a recording chamber mounted on an inverted fluorescence microscope (Leica DMIRB). They were continuously superfused with carbogenated saline (ACSF in mM: NaCl 125, KCl 5,  $\text{NaHCO}_3$  25,  $\text{MgSO}_4$  1.25,  $\text{KH}_2\text{PO}_4$  1.25, glucose 10,  $\text{CaCl}_2$  2.5, pH 7.4 with 5%  $\text{CO}_2$ , and 95%  $\text{O}_2$ ) at 33°C.

### Electrodes and electrochemistry

To obtain stable recordings comprising well-separated exocytotic events in a superfused preparation, stiff CFEs were fabricated (Supplemental Fig. 1). Carbon fibers of 5–7  $\mu\text{m}$  diameter (from Goodfellow, Huntingdon, UK; or Amoco, Greenville, SC, USA, by courtesy of R. H. Chow, University of Southern California) were connected to copper wire using graphite conductive adhesive 112 (EMS, Hatfield, PA, USA). These were inserted and fixed in thin-wall glass capillaries (A-M Systems, Carlsborg, WA, USA) that were pulled on a microelectrode puller (PP-830 Narashige, Japan) to surround the fiber with a glass sleeve of  $\sim 30$ – $50$   $\mu\text{m}$  diameter. To insulate the carbon fiber shaft, the gap between fiber and sleeve was filled with silicon elastomer (Sylgard 184, WPI, Aston, UK) that was cured at 125°C for 48 h. The selectivity of CFEs for detecting a range of oxidizable transmitters—NE, adrenaline, dopamine, ascorbic acid (AA)—and the lack of electroactivity of acetylcholine, reserpine, and amitriptyline were confirmed. Responses to NE as well as spike activity in cultures were tested by amperometry at a range of driving voltages (Supplemental Fig. 1D, E). CFEs were capable of

recording spike activity from individual NEergic release sites in organotypic cultures for up to 2 h without measurable change in spike kinetics. Prior to each recording, CFEs were freshly cut to expose a discoid or short cylindrical carbon surface, and tested by slow cyclic voltammetry (100mV/sec) in ferricyanide solution (1 mM in 0.5M KCl, pH 3; ref. 22). Only cuts displaying smooth, overlaying reduction curves were used for experiments (Supplemental Fig. 1; refs. 22, 23). Maximal reduction currents determined in ferricyanide varied between cuts, depending on the total exposed surface area, but did not correlate with any mean event properties (see below), suggesting that the exposed carbon surface was not a limiting factor to successful oxidation of total transmitter quantity released during single vesicle exocytosis. The CFE was then positioned in the recording chamber using a micro-manipulator (Burleigh PCS-5200, Scientifica, Uckfield, UK), charged to a driving voltage of 800 mV and, under visual control, placed carefully onto a green fluorescent varicosity or soma on the culture surface (Fig. 1A, B; Supplemental Fig. 1C). Because of the possibility of invisible diffusion barriers (fine processes of glial or other non-NEergic cells covering NEergic target structures) or local tissue damage caused by the CFE, any recordings lacking amperometric events, or displaying prominent decrease in spike frequencies over the first 10 min of recording, were discarded.

### Acquisition and analysis of amperometric data

A commercial amplifier (VA-10, npi electronic instruments, Tamm, Germany) driven through a 1401Micro interface by Spike2 software (CED, Cambridge, UK) was used for data acquisition. Recordings were routed through a 50/60Hz noise eliminator (Humbug, Quest Scientific, Digitimer, Welwyn Garden City, UK), filtered at 3 kHz with a 3-pole Bessel low-pass filter, sampled at 3.5 kHz (unless indicated otherwise) and stored for off-line analysis. To detect peaks, and data rising and falling through a threshold level, a semiautomated event recognition routine was developed in script language, using the waveform data analysis algorithms provided by Spike2. The time of beginning, peak, end, half-maximal rise and half-maximal fall of each event was determined and, under individual visual inspection, confirmed or, if necessary, corrected (see Supplemental Fig. 2). Each amperometric spike was characterized by its charge ( $Q$  in pC) derived from the integral, the peak amplitude ( $I_{\text{max}}$  in picoAmpere), and width at half-height ( $t_{1/2}$  in msec) (24). The sd of noise was determined at 0.3–0.4 pA, allowing detection of events with an  $I_{\text{max}}$  from 2–2.5 pA (corresponding to  $\sim 5$ – $10$  pC). Low frequency fluctuations lacking a clear peak and decay phase may reflect NE released at more distant sites and were disregarded. Only events comprising single peaks were included in distribution histograms while events composed of multiple peaks were considered when overall frequencies were determined. Excel (Microsoft) and Prism (Graphpad) were used for downstream data processing. Histograms were compiled and median values were determined for  $I_{\text{max}}$ ,  $t_{1/2}$ , and the cube root of  $Q$  ( $Q^{1/3}$ ). Where appropriate, median values were summarized as averages  $\pm$  SE within groups, and compared between release sites using Student's unpaired two-tailed  $t$  test (24). An estimate of the mean number of molecules oxidized was derived from the average median charge by Equation 1. Equation 1 is based on Faraday's Law, whereby  $Q$  is the charge (in Coulomb),  $n$  the number of electrons involved in the oxidative process (2 for NE), and  $A$  and  $F$  are Avogadro's number and the Faraday constant, respectively (10, 18).

$$(1) \quad \text{molecules} = Q A / n F$$

A putative vesicle diameter was assigned to  $Q$  using Equa-

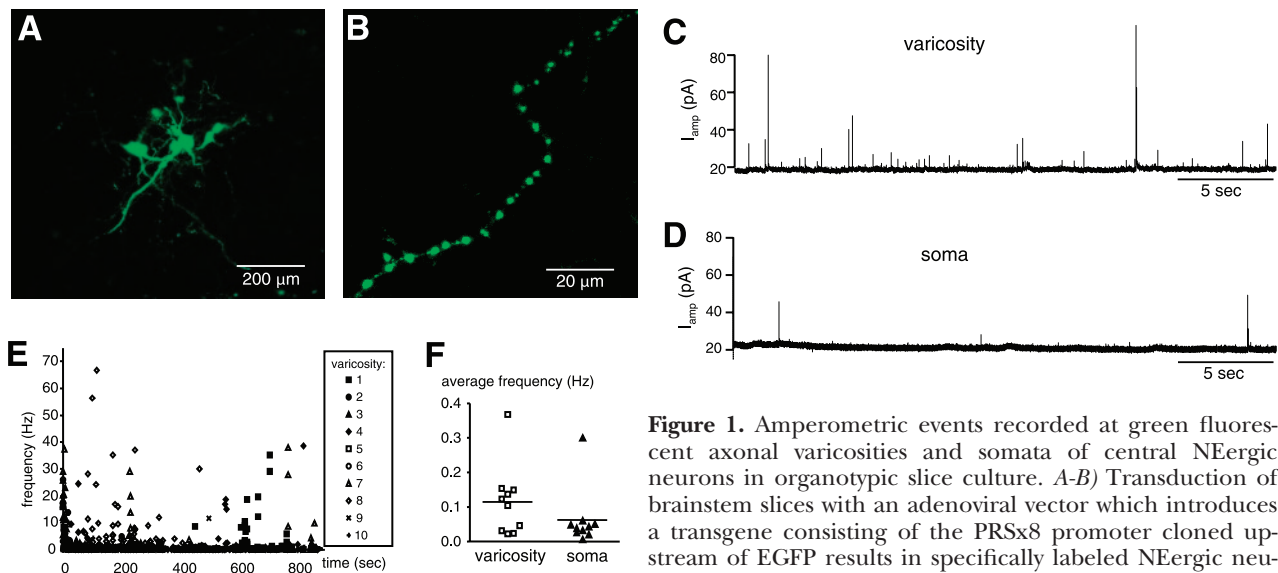


**Figure 1.** Amperometric events recorded at green fluorescent axonal varicosities and somata of central NEergic neurons in organotypic slice culture. *A-B*) Transduction of brainstem slices with an adenoviral vector which introduces a transgene consisting of the PRSx8 promoter cloned upstream of EGFP results in specifically labeled NEergic neurons. *A*) A group of neuronal somata from ventral A1 area

expressing EGFP. Surrounding non-NEergic cells are not labeled. *B*) A single NEergic axon with varicosities, the sites where NE release is expected to occur. *C-D*) Sample recordings from green fluorescent NEergic neurons at a particularly highly release-active varicosity (*C*) and a typical soma (*D*). *E*) Event frequencies, derived from interevent intervals, varied widely between different varicosities and changed spontaneously during recordings. *F*) Scatter plot of average frequencies at varicosity and soma recording sites (10 each; means indicated by horizontal lines). Most varicosities showed higher release frequencies than somata.

tion 2 whereby variables and constants were as in Equation 1 and the intravesicular NE concentration  $C$  (in mol/l) was assumed to be similar to other NEergic cells (10).

$$(2) \text{ vesicle diameter (nm)} = 2 \times 10^8 \times (3Q / 4 \pi n F C)^{1/3}$$

Data from 34 recordings at individual release sites comprising ~2300 single events are presented in this study. These include 20 control recordings (5 each of: A2 varicosities, A2 somata, A1 varicosities, A1 somata), 6 varicosities from reserpine-pretreated cultures (A1 and A2), 3 amitriptyline-pretreated varicosities, and 5 varicosity recordings with tetrodotoxin (TTX). As no differences between the release characteristics from A2 (dorsal) and A1 (ventral) neurons were found, the data were pooled.

## Drugs and reagents

Unless stated otherwise, chemicals and drugs were obtained from Sigma or BDH (VWR International Ltd., Lutterworth, UK), dissolved in water as concentrated stocks, and diluted to the required concentrations immediately before use. TTX (Tocris, Bristol, UK) was diluted in ACSF to 1  $\mu\text{M}$  and applied with the superfusion solution. Reserpine was solved in DMSO or 2 M acetic acid to 10 mM, diluted in culturing media to 10  $\mu\text{M}$ , sterile filtered, and added to cultures at a 500 nM final concentration. Amitriptyline (10 mM in water) was sterile filtered and added to cultures at 10  $\mu\text{M}$  final concentration. Reserpine and amitriptyline were not added to the bath solution during recording.

## RESULTS

### Characteristics of NEergic amperometric spikes

Amperometric oxidation spikes were registered at axonal varicosities as well as at cell bodies of EGFP-

expressing NEergic neurons of A1 and A2 cell groups (Fig. 1*A-D*). The frequency of amperometric events was  $0.091 \pm 0.02$  Hz when averaged over all control recordings ( $n=20$ ). However, spike frequencies varied widely between individual release sites and fluctuated over time during recordings (Fig. 1*E*). For example, at individual sites averaged over a given 5 min period (5–10 min from the initiation of the recording), they ranged from 0.005 to 12.5 Hz. There was a clear trend toward higher release frequencies at axonal as compared to soma release sites (Fig. 1*C, D, F*).

Amperometric events typically had smooth rising and decay phases and covered a wide range of sizes (Fig. 2*A, B*). At most release sites (15 out of 20 control experiments), more complex spike signals comprising multiple peaks and occasional bursts of spikes were registered (Fig. 2*C, D*). Complex events amounted to ~8% of total events registered at soma and varicosity sites. Based on the average event frequencies in these recordings, in most cases complex events could not be explained by a random overlap of independent single release events (24). As complex events did not allow unequivocal resolution of single spike properties, they were excluded from the analysis of quantal release characteristics presented in this study.

### Quantal sizes and kinetics of NE release events

The amount of oxidizable transmitter reaching the electrode following an exocytotic event is related to the registered  $Q$ , which was derived from the spike integral. Histograms of the amperometric charges were strongly skewed to the right, consistent with data reported for other monoaminergic release systems (18, 24, 25).

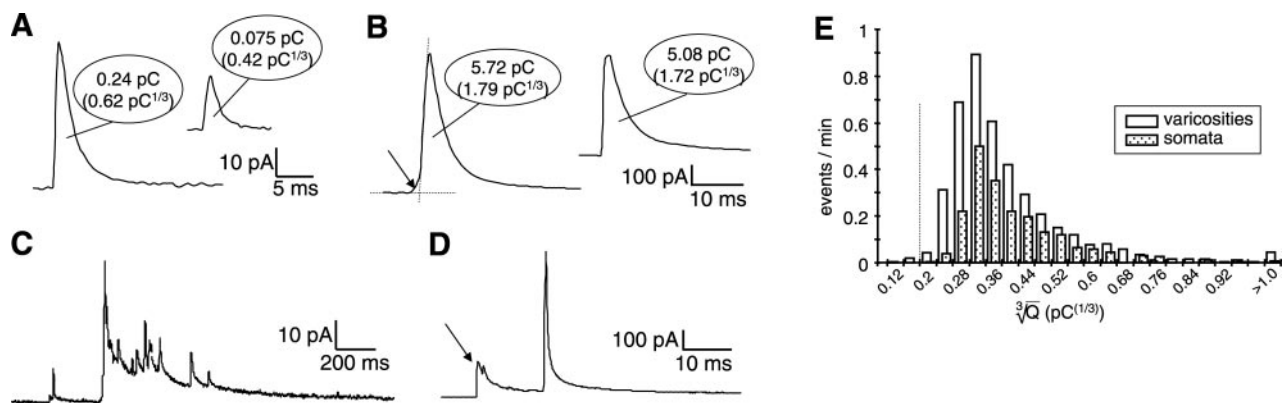


**Figure 2.** Single and complex NE release events in central neurons show a wide range of quantal sizes. *A-B*) Representative amperometric spikes from lower (*A*) and higher (*B*) end of the charge spectrum. Charges (in pC) and their cube roots (in  $\text{pC}^{1/3}$ ) relate to integrals of individual events. Arrow is pointing to a putative short-duration foot signal in the largest event in *B*. Falling phases of these events were better described as 2 phase than 1 phase exponential decay. *C-D*) Complex events were occasionally observed but excluded from further data analysis. *C*) A multi-peaked event occurring in a recording during a background frequency of 0.5 Hz. *D*) A very large event is preceded by a putative foot (arrow) comprising a lower amplitude signal with several peaks and an atypical decay phase. *E*) Cube roots of amperometric charges ( $Q^{1/3}$ ) are thought to be proportional to vesicle diameters. Histograms, pooled for soma (dotted columns) and varicosity (white columns) recordings ( $n=10$  each) and normalized for recording time, reveal a distribution peak at  $\sim 0.04$  pC for both release sites, and reflect lower release frequencies measured at NEergic somata. Note that events in lowest bins (left of dotted line) may be compromised by recording noise but that the distribution declines clearly above that threshold. In addition to the predominant population of events, larger quanta which make a  $>30\%$  contribution to total NE release are found mainly at varicosities.

Conversion of charges into cube roots ( $Q^{1/3}$ ) to accommodate for catecholamine storage within spherical vesicles revealed two major populations of quanta (Fig. 2*E* and Fig. 3). At single release sites, the predominant population of events was well described by a Gaussian

distribution (Fig. 3*A*). The average median amperometric charge of this population was  $0.04 \pm 0.003$  pC and the median  $I_{\max}$   $8.5 \pm 0.4$  pA ( $n=20$  release sites). These values were not significantly different between soma and axonal release sites ( $n=10$  each; Fig. 3*B, C*).

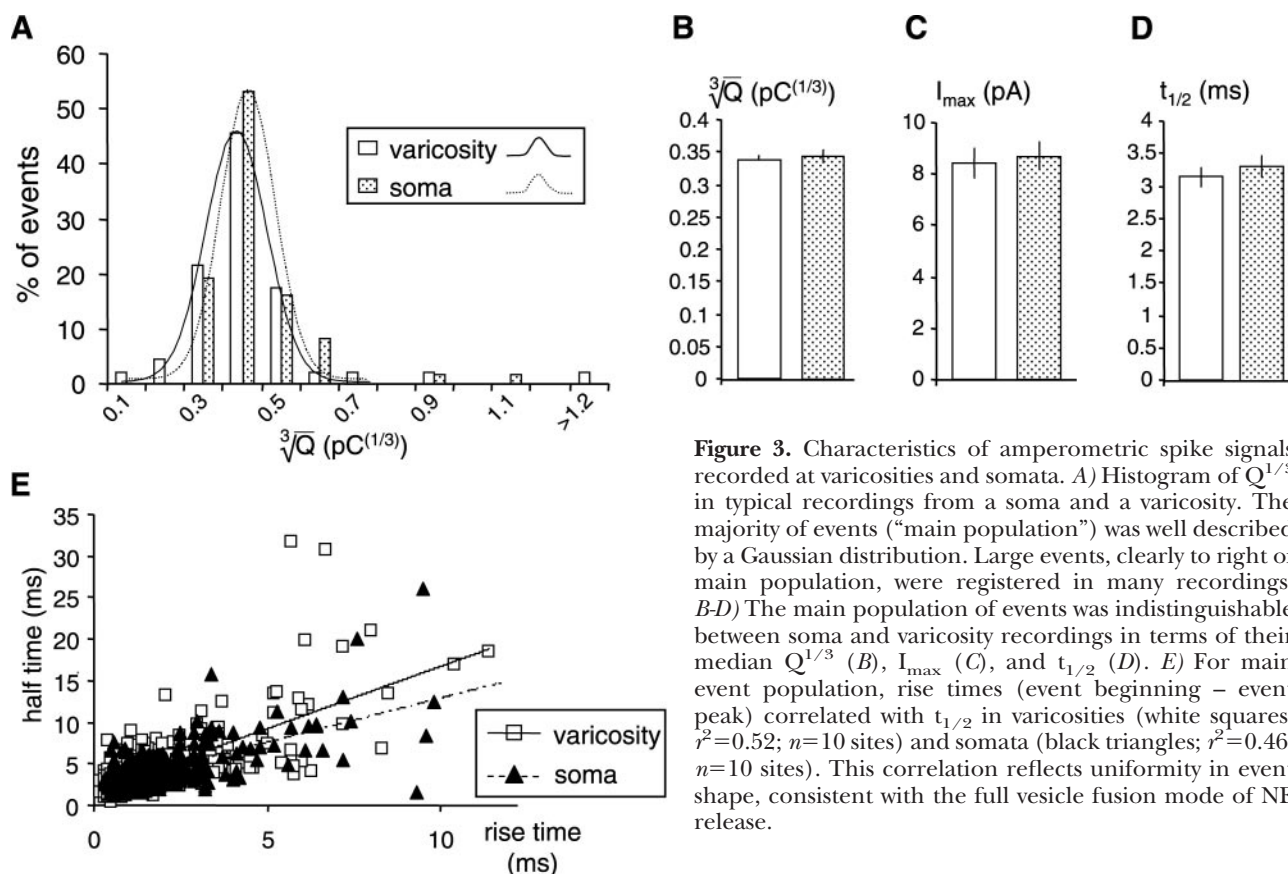


**Figure 3.** Characteristics of amperometric spike signals recorded at varicosities and somata. *A*) Histogram of  $Q^{1/3}$  in typical recordings from a soma and a varicosity. The majority of events ("main population") was well described by a Gaussian distribution. Large events, clearly to right of main population, were registered in many recordings. *B-D*) The main population of events was indistinguishable between soma and varicosity recordings in terms of their median  $Q^{1/3}$  (*B*),  $I_{\max}$  (*C*), and  $t_{1/2}$  (*D*). *E*) For main event population, rise times (event beginning – event peak) correlated with  $t_{1/2}$  in varicosities (white squares;  $r^2=0.52$ ;  $n=10$  sites) and somata (black triangles;  $r^2=0.46$ ;  $n=10$  sites). This correlation reflects uniformity in event shape, consistent with the full vesicle fusion mode of NE release.

This population of events had an average median  $t_{1/2}$  of  $3.2 \pm 0.12$  ms ( $n=20$ ) which, again, was not different between varicosities and somata (Fig. 3D). For individual events,  $t_{1/2}$  was correlated with rise time (Fig. 3E;  $r^2=0.52$  for varicosities;  $r^2=0.46$  for somata) but not with  $I_{\max}$  ( $r^2<0.001$ ) and only weakly with  $Q$  ( $r^2<0.16$ ; data not shown). Less than 0.5% of single events in the main population appeared to have foot signals characterized by slow, lower amplitude currents preceding the rapid upstroke of a typical amperometric spike (Fig. 2), indicating that prolonged fusion pore opening is not a preferred mechanism of release from the bulk of central NEergic vesicles.

The second population consisted of much larger release events with charges far to the right of the main population ( $Q>0.5$  pC; Figs. 2B, E and 3A). The  $Q^{1/3}$  values of these events were not normally distributed but spread broadly across the range (0.5–5.7 pC). They had an average charge of 1.45 pC, an average  $I_{\max}$  of 146 pA (range 18–748 pA), and a  $t_{1/2}$  of  $5.1 \pm 0.3$  ms ( $n=24$ ). Events of this kind were  $\sim 3$  times more frequent at axonal release sites (18 events at 9 out of 10 sites) as opposed to somata (6 events at 4 out of 10 sites). Some of the largest events encountered in this spectrum ( $>1.7$  pC) were not included in the evaluation because they were part of complex events and therefore insufficiently well separated from preceding or following signals. Of these, at least eight were identified at axonal and only one at a somatic release site. Several of the large events were preceded by foot-like signals (arrows in Fig. 2B, D).

The total amperometric charge integrated over a spike can be directly related to the number of oxidized transmitter molecules (see Materials and Methods, Equation 1; refs. 10, 18). Thus, the detected main vesicle population corresponds to an average release of  $1.13 \times 10^5 - 1.3 \times 10^5$  molecules of oxidizable transmitter (derived from average  $Q \pm SE$ ; see Materials and Methods, Equation 1). In contrast, during one large event, on average  $3.63 \times 10^6$  to  $5.4 \times 10^6$  molecules were detected. Although large ( $>0.5$  pC) events represented  $<2\%$  of all simple spikes under normal conditions, because of their high charge, they contributed with  $>35\%$  to the total release of NE from varicosities (Fig. 4). On somata, their contribution amounted to only 25% (Fig. 4).

Central dopaminergic release events were reported to have considerably faster kinetics ( $t_{1/2} \sim 0.12-0.2$  ms) than the NEergic events we recorded (23, 26–28). We therefore attempted to unmask any ultrashort spikes by increasing the sampling frequency to 10 kHz and removing any filtering but revealed no additional events ( $n=3$ , data not shown).

### Action potential activity and release event frequency

To determine to what extent release events were triggered by spontaneous action potential activity in slice cultures, 1  $\mu$ M TTX was added to the superfusion solution. At this concentration TTX completely blocks action potential generation within less than two minutes in slice cultures kept under similar conditions (S. Wang and S. Kasparov,

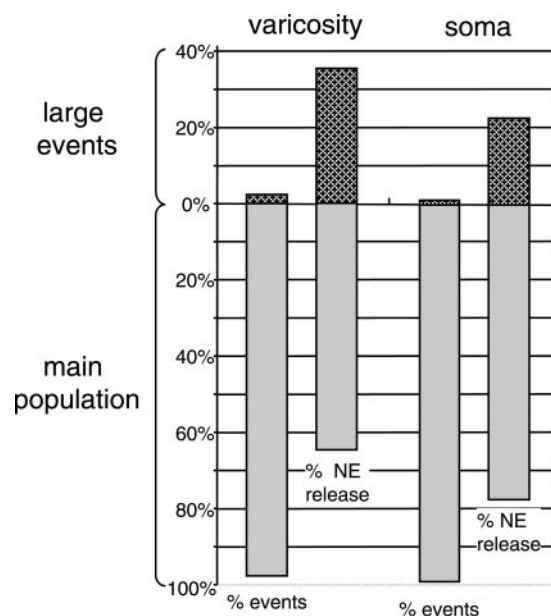


**Figure 4.** Large events contribute a considerable proportion of total NE release. Events exceeding 0.5 pC (hatched columns on top) made up a small fraction of all registered simple events (2.3% for varicosities; 1.5% for somata) but represented a significant proportion of the total amperometric charge (35% at varicosities; 25% at somata). Thus, large events were more abundant and had higher charges in varicosities as compared to somata.

personal communication). After 1–3 min of exposure to TTX the number of release events at varicosities was markedly reduced (on average to  $\sim 30\%$  of control) but they were not completely abolished (Fig. 5). Despite the decrease in overall event frequency in TTX, the relative occurrence of big events (2.9%) and complex events (8%) was very similar to control. The effects of TTX were partially reversed after  $\sim 10$  min of washing.

### Effects of reserpine and amitriptyline on NEergic quantal size distribution

Pretreatment with the vesicular monoamine transporter inhibitor reserpine (500 nM for  $>24$  h) significantly decreased the average event frequency at varicosities to  $0.03 \pm 0.005$  Hz ( $n=6$ ;  $P<0.05$ ; Fig. 6A). When expressed as average charge per minute, this resulted in a decrease in total transmitter released by varicosities to  $\sim 50\%$ . At the same time, reserpine slightly increased  $I_{\max}$  (to  $10.6 \pm 1.4$  pA; Fig. 6B) and  $t_{1/2}$  (to  $3.3 \pm 0.46$  ms; Fig. 6C) which resulted in a higher median  $Q$  ( $0.052 \pm 0.003$  pC; Fig. 6D;  $P<0.02$ ). This may be explained by the preferential loss of events with lower charges ( $<0.4$  pC $^{1/3}$ ; Fig. 6E). Large events ( $>0.5$  pC) were still evident in reserpine-treated varicosities, and their relative abundance and average NE content appeared unaffected (Fig. 6G).

In contrast, amitriptyline pretreatment (10  $\mu$ M for 1 wk;  $n=3$ ) did not affect average frequencies (Fig. 6A) and did not change significantly the median  $I_{\max}$  of the main population (Fig. 6B). However, both median  $t_{1/2}$  and  $Q$  were profoundly increased ( $P<0.02$  and  $<0.01$ , respec-

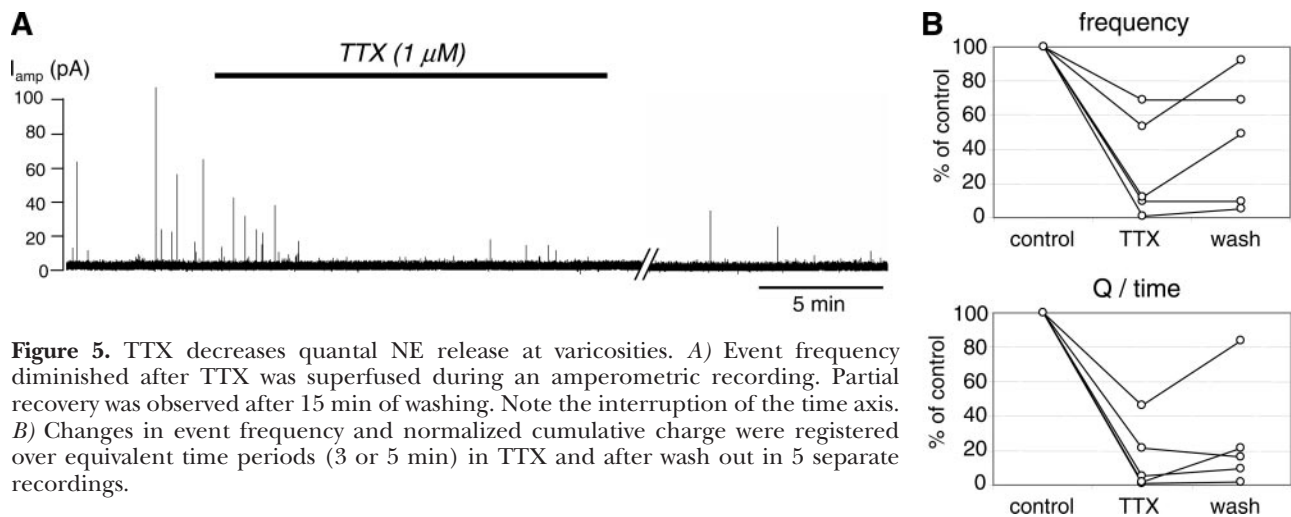


**Figure 5.** TTX decreases quantal NE release at varicosities. *A*) Event frequency diminished after TTX was superfused during an amperometric recording. Partial recovery was observed after 15 min of washing. Note the interruption of the time axis. *B*) Changes in event frequency and normalized cumulative charge were registered over equivalent time periods (3 or 5 min) in TTX and after wash out in 5 separate recordings.

tively; Fig. 6*C-D, F*). This amounted to a 180% increase in average  $Q$  per minute compared to untreated varicosities. The frequency of large events as well as their quantal size slightly increased (both by 5%) so that their contribution totaled 44% of overall NE release (Fig. 6*G*).

## DISCUSSION

To our knowledge this study is the first to describe characteristics of quantal release of NE from central neurons. We found that exocytosis of NE in the brain

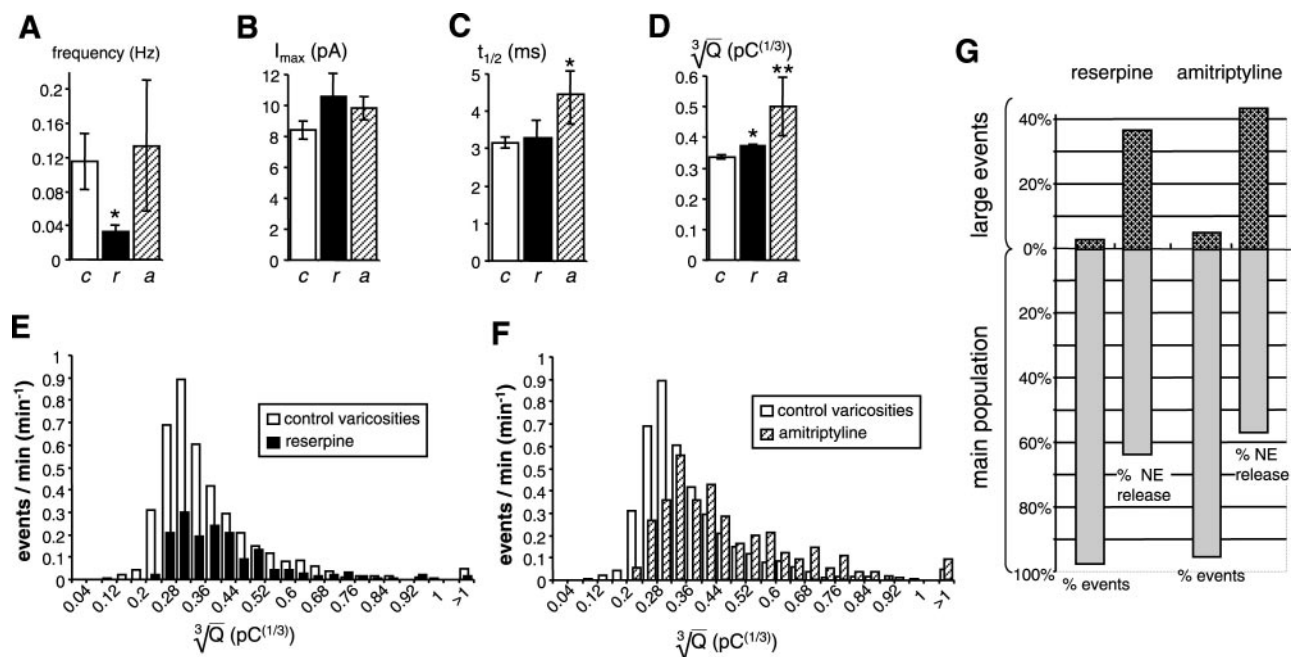


**Figure 6.** Effect of reserpine and amitriptyline pretreatment on quantal NA release from varicosities. *A*) Average release frequency was significantly reduced at varicosity release sites in reserpine-treated ( $r$ ;  $n=6$ ;  $P<0.05$ , Student's  $t$  test for samples with unequal variance; normality test passed in Prism) but not in amitriptyline-treated ( $a$ ;  $n=3$ ) slices as compared to control ( $c$ ;  $n=10$ ). *B*) Median event amplitudes were only slightly increased after reserpine and amitriptyline treatment, statistical significance was not reached. *C*) Events were significantly broadened by amitriptyline ( $P<0.02$ ) but not by reserpine. *D*) Quantal size, as represented by median  $Q^{1/3}$ , was significantly increased following reserpine ( $P<0.02$ ) and profoundly increased following amitriptyline ( $P<0.01$ ) treatment. *E*) Quantal distribution ( $Q^{1/3}$ ) of events pooled from reserpine-treated varicosities (black columns;  $n=6$ ) and normalized for recording time, in comparison to control (white columns;  $n=10$ ). Reserpine decreased quantal release per unit time to 54% of control and particularly affected smaller quanta at the lower end of the spectrum, explaining the net increase in median quantal size (*D*). *F*) Quantal distribution ( $Q^{1/3}$ ) of events pooled from amitriptyline-treated varicosities (hatched columns;  $n=3$ ) and normalized for recording time, in comparison to control (white columns;  $n=10$ ). Amitriptyline increased quantal release per unit time to 180% of control by increasing quantal sizes across the spectrum. *G*) For events exceeding 0.5 pC ( $\sim 0.8$  pC $^{1/3}$ ; hatched column fractions on top) event frequencies and NE contribution were similar to control values in reserpine-treated slices (left columns; compare Fig. 4) but were increased to >5% of events contributing  $\sim 44\%$  of total NE release in amitriptyline-treated varicosities (right hand columns).

occurs in at least two disparate quantal size ranges, an abundant population of medium-sized quanta and infrequent large quanta, comparable in size with chromaffin granule exocytosis. The majority of release events are dissimilar to those found in both, bovine chromaffin cells and central dopaminergic neurons. They have kinetics consistent with the full fusion model of release. Further, NE is released from axonal varicosities as well as somata and the distribution of quantal sizes is different between the two compartments. Neuronal firing plays a role in driving NE release, but even in absence of action potential drive spontaneous release events are detectable, suggesting that release sites may autonomously regulate their activity.

The PRSx8 promoter that we use to drive EGFP expression, with few exceptions, operates specifically in NEergic and adrenergic neurons (20, 21). EGFP expression in our slice cultures was restricted to the locations corresponding to A2 neurons in the nucleus of the solitary tract and the ventral A1 group (29). EGFP-labeled varicose axons migrate throughout the cultures and preferentially along the slice edges (15; Fig. 1*B*). Transcriptional activity of PRSx8 has also been found in some cholinergic cell groups (20), but acetylcholine is not detected by amperometry. In contrast, AA is electroactive. It is involved in intravesicular NE synthesis and was reported to be costored in chromaffin cell granules at ~5% of the catecholamine concentration (30, 31). This may be similar in some central NEergic cell groups (30). Therefore, although the events registered in the present study evidently reflect quantal release of NE, we acknowledge that coreleased AA might have contributed to the amperometric signals.

The two brainstem NE-releasing cell groups investigated, A1 and A2, showed indistinguishable release characteristics and are therefore discussed together. To assume a uniform release mechanism for all central NEergic neurons may, however, be an oversimplification. Considering the multitude of functions and projection targets (reviewed in 32), NEergic neurons from different cell groups may well have different release characteristics that remain to be studied.

In this study, we analyzed spontaneously occurring vesicle fusion events in the brainstem slice culture. We know from whole-cell patch clamp experiments in this preparation that the majority of NEergic neurons fire spontaneous action potentials (Supplemental Fig. 3). For example, of 12 neurons (6 each of areas A1 and A2), 3 were quiescent, 4 produced single action potentials at varying intervals (average 3.6 Hz; range 0.7–11.5 Hz), and 5 fired in bursts of 0.01–1.1 Hz. Peak firing frequencies of 5–40 Hz were reached during bursts (A. G. Teschemacher and Z. Chiti, data not shown). Thus, the variability in amperometric event frequencies between different release sites and during recordings is overall consistent with action potential activity of NE neurons under our recording conditions. The prominent reduction of amperometric signals in TTX demonstrates the importance of propagating action potentials for con-

trol of central NE exocytosis but also suggests a role for action potential-independent release.

### Central NEergic vesicle populations

EM studies of the mammalian brain revealed two predominant NE-containing vesicle types: A small clear (40–60 nm in diameter) and a slightly larger dense core (80–120 nm) variety (4–6). To relate vesicle diameter to quantal size, the intravesicular NE concentration is required, which is, however, presently not known for central NEergic neurons (see Materials and Methods, Equation 2). For adrenal chromaffin large dense core granules, catecholamine concentrations ranging between 0.11 and 2.5 M have been derived from combined amperometry-capacitance or amperometry-morphometric measurements (9, 10, 18, 33, 34). Taking the proposed NE contents of chromaffin granules as a point of reference, and assuming an intravesicular NE concentration of ~0.4 M, our main quantal population (~ $1.2 \times 10^5$  NE molecules/quantum; see Materials and Methods, Equation 1) is distributed around a mean diameter of 99 nm that ties up well with the central dense core vesicle population found with EM (80–120 nm; see Materials and Methods, Equation 2). If small clear NEergic vesicles (40–60 nm) are release-active, higher intravesicular NE concentrations seem more likely. Loaded with ~1 M NE, exocytosis of ~45–55 nm diameter vesicles would release  $\sim 3.1\text{--}4.7 \times 10^4$  molecules, corresponding to events in the 0.24 pC<sup>1/3</sup> bin toward the lower end of our main quantal population (Fig. 2*E*; see Materials and Methods, Equations 1, 2). Detection of events from vesicles <40 nm and/or containing <0.5 M NE would have been compromised due to signal-to-noise levels (see Materials and Methods). As intravesicular NE loading of vesicles is a dynamic process that depends on catecholamine uptake and metabolism, a broad concentration range would be expected within actively signaling tissue. We therefore propose that our main quantal population represents release from both, small clear and dense core vesicles, ranging between 40 and 120 nm in diameter with intravesicular NE concentrations between 0.4 and 1 M (Fig. 7).

In contrast, the large, predominantly axonal, release events are consistent with large vesicles of around 300 nm diameter containing ~0.5 M NE, which compares to chromaffin granule size and catecholamine load (9). The large variability in their charges may reflect differences in NE content while their lower frequency may result from a limited pool size. In fact, recent EM studies have identified large dense core vesicles in the rodent brain and have implied that exocytosis should be a comparatively rare incident (35). Alternatively, the large signals may originate from compound exocytosis where several vesicles combine prior to fusing with the plasma membrane (10). Large events outside of the main population have also been reported for central dopamine release although they were noticeably smaller than the largest events registered here (23, 26). Although attempts to amperometrically detect quantal

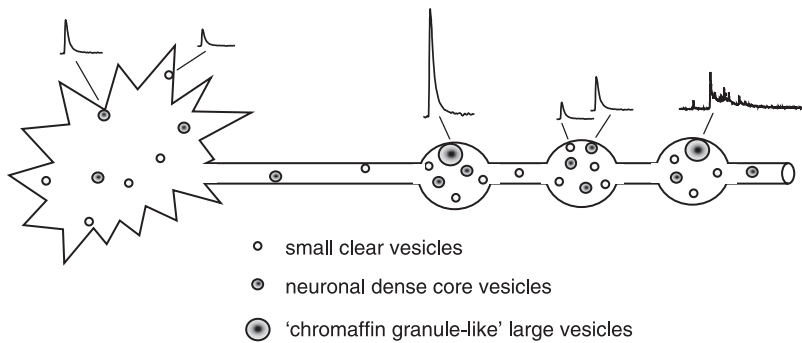


**Figure 7.** Hypothesized distribution of NE-containing secretory vesicles, release sites, and modes of release in central neurons. Small clear (light centered) and dense core (dark centered) vesicles undergo exocytosis at soma and varicosities. Exocytosis of large vesicles with NE contents comparable to chromaffin cell granules results in high NE output, predominantly at axonal varicosities. These vesicles produce large unitary events or, alternatively, may undergo sequential partial release in a flickering-fusion-pore fashion.

NE release from sympathetic neurons *in situ* were unsuccessful in the past (36), one study in dissociated cultured superior cervical ganglion neurons (37) has reported events with a quantal size in the same order of magnitude and a similar time course as compared to the main population in our report. Large events were not described.

As examples of peptidergic and serotonergic neurons show, presence of multiple types of secretory vesicles may have important implications for the downstream effects of released transmitter and cotransmitters (38, 39). Exocytosis of different vesicle categories may also be differentially regulated (38, 39).

#### Kinetics of central NE vesicle release – “foot signals” and time course

The  $t_{1/2}$  of NEergic release spikes was remarkably similar between small (3.2 ms) and large events (5 ms). Although comparable in terms of the  $I_{max}$ , the main population of NE currents had markedly slower kinetics than central dopamine release events (23, 26) and this was not due to filtering or sampling frequency differences. On the other hand, while in terms of quantal size, large release events in central NEergic neurons were comparable to chromaffin granule exocytosis, their time courses were notably faster (~4–20 times; refs. 9, 10, 33, 40–43). Our recordings were carried out at 33°C, while the majority of chromaffin cell studies were performed at ambient temperature. Higher temperatures slightly decrease spike half-widths in chromaffin cells (44), but from our earlier recordings using commercially available CFEs we know that at ambient temperature NE release events are not markedly longer ( $t_{1/2}$  ~5 ms; ref. 17). Therefore, differences in the recording temperatures cannot account for the faster kinetics of quantal release in central NEergic neurons as compared to chromaffin cells, suggesting a fundamental difference in the molecular mechanisms of NE exocytosis. In bovine chromaffin cells, NE is complexed by the vesicular matrix that expands after fusion pore formation, leading to a postfusion delay in transmitter release (11, 41, 45, 46). Shorter events in brain NEergic neurons would therefore be consistent with a lower intravesicular chromogranin A content as shown for NEergic vesicles in postganglionic sympathetic neurons (47).

Foot signals are commonly observed in chromaffin cells where they are thought to result from transmitter diffusion through a fusion pore prior to full fusion. Transmitter release through transiently forming fusion pores also underlies the so-called “kiss-and-run” exocytosis in chromaffin cells (9, 33, 42, 48). Foot-only events, like foot signals, in chromaffin cells vary in length depending on the duration of fusion pore openings (9, 33). Recent evidence suggested that central dopaminergic vesicles can partially release their contents during fusion pore flickering, resulting in complex multi-peaked amperometric events (27). The lack of foot signals in our main event population indicates that full fusion is the key mechanism of transmitter release by small clear and dense core vesicles in central NEergic neurons. This population of events shows a fairly homogenous distribution of durations (Fig. 3A) and is, furthermore, compatible with morphometrically determined predominant vesicle types in the brain. Therefore, our evidence does not support the hypothesis that the main population of events are due to “kiss-and-run” release from large-quantum vesicles.

In contrast, some of the large NE release events in our recordings have foot-like signals similar to chromaffin granule exocytosis. The largest spikes were often preceded by a volley of lower peaks or embedded in a complex event. Since complex events persisted in the presence of TTX, they are unlikely to represent multiple fusion events triggered by high frequency bursts of action potentials. An alternative explanation is that, like dopaminergic central vesicles and chromaffin granules, large vesicles may sequentially release their content during reversible pore openings (see Fig. 7).

#### Modulation of quantal sizes

The tricyclic antidepressant amitriptyline is a known inhibitor of central NE and serotonin reuptake. One of its acute effects, therefore, includes an increase in extracellular NE levels in the brain (49). However, clinical effects of amitriptyline take several weeks to develop. Therefore, while the mechanisms underlying its antidepressant action or the range of adverse side effects are currently not well understood, they are thought to involve adaptational processes and synaptic plasticity (50). We found a prominent increase in

quantal size, which was mainly due to a prolonged  $t_{1/2}$ . This is consistent with a higher NE content within vesicles which, in turn, could call for an adaptation in intravesicular NE storage matrix to accommodate for the higher intravesicular NE concentrations. Intravesicular matrix is thought to underlie delayed release of catecholamine from fused chromaffin granules (45, 51). In support of a delayed release mechanism, we found that median rising and falling phases of events were lengthened to >150 and 250%, respectively, by amitriptyline. Further, while NE contents of single large events after amitriptyline were only slightly increased over control values, they were increased in frequency, in line with relative abundance of releasable NE, and also showed slowed kinetics. In our experiments, cultures were pretreated with amitriptyline but recorded while being superfused with normal bath solution. Nevertheless, residual amitriptyline might have not been completely washed out from the tissue before recording. Therefore, protracted presence of NE in the extracellular space due to an inhibited reuptake mechanism may have contributed to the longer  $t_{1/2}$ .

In contrast to amitriptyline, reserpine interferes with vesicular NE storage and affects mood negatively (49, 50). Reserpine has been shown to reduce quantal size and suppress release in adrenal chromaffin cells, the PC12 cell line, and central dopaminergic neurons (26, 52, 53). In our experiments, reserpine profoundly affected the main population of release events and predominantly depleted the smallest quanta. Could reserpine-resistant events be explained by continued release of an oxidizable cotransmitter from NE-depleted vesicles? Whereas AA is known to be coreleased with NE from chromaffin cells, the intravesicular AA concentration was estimated at more than an order of magnitude lower than for catecholamines (31). Therefore, one would rather expect reserpine to decrease the average quantal size but not the total event frequency, making this explanation implausible. On the other hand, it has long since been known that, while reserpine severely decreases brain NE, it does not completely deplete it (54). Hence it is more likely that distinct types of NEergic vesicles in neurons differ in their sensitivity to reserpine. Differential expression of vesicular monoamine transporter isoforms on different vesicle populations in central catecholaminergic neurons may underlie such an effect (4, 5, 55). Therefore, a possible explanation for the action of reserpine in our experiments is the preferential depletion of NE from small vesicles.

### NE release from different neuronal compartments

We demonstrate for the first time that NEergic neurons from areas A1 and A2 release transmitter not only from soma-remote axons but also from their cell bodies (Fig. 7). While axonal varicosities were the conventionally accepted sites of release, NE as well as its synthesizing enzyme, dopamine- $\beta$ -hydroxylase are present throughout NEergic neurons (32). Over the recent years,

somato-dendritic release has been described for a range of central transmitters, including dopamine and neuropeptides (23, 28, 56, 57). Quantal release of dopamine from cell bodies of substantia nigra neurons was unequivocally demonstrated using a similar single-cell amperometric approach (23). Regarding NE, several previous lines of evidence pointed to the existence of regulated NE release from somato-dendritic compartments. For example, NE fluctuations were electrochemically detected in areas of high density of NEergic cell bodies (58). Further, EM data suggested the existence of dendro-dendritic synapses in the locus coeruleus (7). The fact that large events described in this study are much more frequent at axonal release sites may indicate that somato-dendritic and axonal release could be differentially regulated. This could have important physiological implications because NE released from the somato-dendritic compartment is likely to be primarily involved in autocrine negative feedback.

In conclusion, central NE release shows unique characteristics that set it apart from other catecholamine-secreting cells in brain and periphery. Further studies will clarify the mechanisms controlling NE release probability at the level of individual release sites and establish whether these are different between axonal varicosities and neuronal somata. FJ

We thank Drs. S. Kasparov and J. Millar, and J. F. R. Paton for valuable discussions and encouragement, J. Vinicombe and J. Croker for technical support and N. Nikiforova and T. Saunders for technical assistance. This work was supported by the British Heart Foundation (FS/04/003 to A. G. T.), the Wellcome Trust (VIP award to Z. C.), and the Royal Society (2004/R1 to A. G. T.).

### REFERENCES

1. Singewald, N., and Philippu, A. (1996) Involvement of biogenic amines and amino acids in the central regulation of cardiovascular homeostasis. *Trends Pharm. Sci.* **17**, 356–363
2. Olson, V. G., Heusner, C. L., Bland, R. J., During, M. J., Weinschenker, D., and Palmiter, R. D. (2006) Role of noradrenergic signaling by the nucleus tractus solitarius in mediating opiate reward. *Science* **311**, 1017–1020
3. Sulzer, D., and Edwards, R. H. (2005) Antidepressants and the monoamine masquerade. *Neuron* **46**, 1–2
4. Pickel, V. M., Nirenberg, M. J., and Milner, T. A. (1996) Ultrastructural view of central catecholaminergic transmission: immunocytochemical localization of synthesizing enzymes, transporters and receptors. *J. Neurocytol.* **25**, 843–856
5. Nirenberg, M. J., Liu, Y., Peter, D., Edwards, R. H., and Pickel, V. M. (1995) The vesicular monoamine transporter 2 is present in small synaptic vesicles and preferentially localizes to large dense core vesicles in rat solitary tract nuclei. *Proc Natl. Acad. Sci. U.S.A.* **92**, 8773–8777
6. Bloom, F. E., and Aghajanian, G. K. (1968) An electron microscopic analysis of large granular synaptic vesicles of the brain in relation to monoamine content. *J. Pharmacol. Exp. Ther.* **159**, 261–273
7. Groves, P. M., and Wilson, C. J. (1980) Monoaminergic presynaptic axons and dendrites in rat locus coeruleus seen in reconstructions of serial sections. *J. Comp. Neurol.* **193**, 853–862
8. Egan, T. M., Henderson, G., North, R. A., Williams, J. T. (1983) Noradrenaline-mediated synaptic inhibition in rat locus coeruleus neurones. *J. Physiol.* **345**, 477–488

9. Albillos, A., Dernick, G., Horstmann, H., Almers, W., Alvarez de Toledo, G., and Lindau, M. (1997) The exocytotic event in chromaffin cells revealed by patch amperometry. *Nature* **389**, 509–512
10. Wightman, R. M., Jankowski, J. A., Kennedy, R. T., Kawagoe, K. T., Schroeder, T. J., Leszczyszyn, D. J., Near, J. A., Diliberto, E. J., Jr., Viveros, O. H. (1991) Temporally resolved catecholamine spikes correspond to single vesicle release from individual chromaffin cells. *Proc Natl. Acad. Sci. U.S.A* **88**, 10754–10758
11. Wightman, R. M., Troyer, K. P., Mundorf, M. L., and Catahan, R. (2002) The association of vesicular contents and its effects on release. *Ann. N.Y. Acad. Sci.* **971**, 620–626
12. Neher, E. (1998) Vesicle pools and Ca<sup>2+</sup> microdomains: new tools for understanding their roles in neurotransmitter release. *Neuron* **20**, 389–399
13. Rettig, J., and Neher, E. (2002) Emerging roles of presynaptic proteins in Ca<sup>++</sup>-triggered exocytosis. *Science* **298**, 781–785
14. Teschemacher, A. G. (2005) Real-time measurements of noradrenaline release in periphery and central nervous system. *Auton. Neurosci.* **117**, 1–8
15. Teschemacher, A. G., Paton, J. F., and Kasparov, S. (2005) Imaging living central neurones using viral gene transfer. *Adv. Drug Del. Rev.* **57**, 79–93
16. Teschemacher, A. G., Wang, S., Lonergan, T., Duale, H., Waki, H., Paton, J. F., and Kasparov, S. (2005) Targeting specific neuronal populations in the rat brainstem using adeno- and lentiviral vectors: applications for imaging and studies of cell function. *Exper. Physiol.* **90**, 61–69
17. Teschemacher, A. G. (2004) Microamperometric recording of noradrenaline release from visualised axonal varicosities of A1 noradrenergic neurones. *J. Physiol.* **555P**, C40
18. Travis, E. R., and Wightman, R. M. (1998) Spatio-temporal resolution of exocytosis from individual cells. *Annu. Rev. Biophys. Biomol. Struct.* **27**, 77–103
19. Teschemacher, A. G., and Seward, E. P. (2000) Bidirectional modulation of exocytosis by angiotensin II involves multiple G-protein-regulated transduction pathways in chromaffin cells. *J. Neurosci.* **20**, 4776–4785
20. Lonergan, T., Teschemacher, A. G., Hwang, D. Y., Kim, K.-S., Pickering, A. E., and Kasparov, S. (2005) Targeting brain stem centers of cardiovascular control using adenoviral vectors: Impact of promoters on transgene expression. *Physiol. Genom.* **20**, 165–172
21. Hwang, D. Y., Carlezon, W. A., Jr., Isacson, O., and Kim, K. S. (2001) A high-efficiency synthetic promoter that drives transgene expression selectively in noradrenergic neurons. *Hum. Gene Ther.* **12**, 1731–1740
22. Schulte, A., and Chow, R. H. (1996) A simple method for insulating carbon-fiber microelectrodes using anodic electrophoretic deposition of paint. *Anal. Chem.* **68**, 3054–3058
23. Jaffe, E. H., Marty, A., Schulte, A., and Chow, R. H. (1998) Extrasynaptic vesicular transmitter release from the somata of substantia nigra neurons in rat midbrain slices. *J. Neurosci.* **18**, 3548–3553
24. Mosharov, E. V., and Sulzer, D. (2005) Analysis of exocytotic events recorded by amperometry. *Nature Meth.* **2**, 651–658
25. Finnegan, J. M., Pihel, K., Cahill, P. S., Huang, L., Zerby, S. E., Ewing, A. G., Kennedy, R. T., and Wightman, R. M. (1996) Vesicular quantal size measured by amperometry at chromaffin, mast, pheochromocytoma, and pancreatic beta-cells. *J. Neurochem.* **66**, 1914–1923
26. Pothos, E. N., Davila, V., and Sulzer, D. (1998) Presynaptic recording of quanta from midbrain dopamine neurons and modulation of the quantal size. *J. Neurosci.* **18**, 4106–4118
27. Staal, R. G., Mosharov, E. V., and Sulzer, D. (2004) Dopamine neurons release transmitter via a flickering fusion pore. *Nature Neurosci.* **7**, 341–346
28. Puopolo, M., Hochstetler, S. E., Gustincich, S., Wightman, R. M., and Raviola, E. (2001) Extrasynaptic release of dopamine in a retinal neuron: activity dependence and transmitter modulation. *Neuron* **30**, 211–225
29. Paxinos, G., and Watson, C. (1986) *The Rat Brain in Stereotaxic Coordinates*. Academic Ltd., London, UK
30. Grünewald, R. A. (1993) Ascorbic acid in the brain. *Brain Res. Brain Res. Rev.* **18**, 123–133
31. Winkler, H., and Westhead, E. (1980) The molecular organization of adrenal chromaffin granules. *Neuroscience* **5**, 1803–1823
32. Fillenz, M. (1990) *Noradrenergic Neurons*. Cambridge Univ. Press, Cambridge, UK
33. Ales, E., Tabares, L., Poyato, J. M., Valero, V., Lindau, M., and Alvarez de Toledo, G. (1999) High calcium concentrations shift the mode of exocytosis to the kiss-and-run mechanism. *Nature Cell Biol.* **1**, 40–44
34. Grabner, C. P., Price, S. D., Lysakowski, A., and Fox, A. P. (2005) Mouse chromaffin cells have two populations of dense core vesicles. *J. Neurophysiol.* **94**, 2093–2104
35. Crivellato, E., Nico, B., and Ribatti, D. (2005) Ultrastructural evidence of piecemeal degranulation in large dense-core vesicles of brain neurons. *Anat. Embryol.* **210**, 25–34
36. Stjärne, L. (2000) Do sympathetic nerves release noradrenaline in “quanta”? *J. Auton. Nerv. Syst.* **81**, 236–243
37. Zhou, Z., and Mislser, S. (1995) Amperometric detection of stimulus-induced quantal release of catecholamines from cultured superior cervical ganglion neurons. *Proc Natl. Acad. Sci. U.S.A* **92**, 6938–6942
38. Klyachko, V. A., and Jackson, M. B. (2002) Capacitance steps and fusion pores of small and large-dense-core vesicles in nerve terminals. *Nature* **418**, 89–92
39. Bruns, D., Riedel, D., Klingauf, J., and Ahn, R. (2000) Quantal release of serotonin. *Neuron* **28**, 205–220
40. Schroeder, T. J., Jankowski, J. A., Kawagoe, K. T., Wightman, R. M., Lefrou, C., and Amatore, C. (1992) Analysis of diffusional broadening of vesicular packets of catecholamines released from biological cells during exocytosis. *Anal. Chem.* **64**, 3077–3083
41. Jankowski, J. A., Schroeder, T. J., Ciolkowski, E. L., and Wightman, R. M. (1993) Temporal characteristics of quantal secretion of catecholamines from adrenal medullary cells. *J. Biol. Chem.* **268**, 14694–14700
42. Amatore, C., Arbault, S., Bonifas, I., Bouret, Y., Erard, M., Ewing, A. G., and Sombers, L. A. (2005) Correlation between vesicle quantal size and fusion pore release in chromaffin cell exocytosis. *Biophys. J.* **88**, 4411–4420
43. Chow, R. H., von Ruden, L., and Neher, E. (1992) Delay in vesicle fusion revealed by electrochemical monitoring of single secretory events in adrenal chromaffin cells. *Nature* **356**, 60–63
44. Walker, A., Glavinovic, M. I., and Trifaro, J. (1996) Temperature dependence of release of vesicular content in bovine chromaffin cells. *Plügers Archiv. – Euro. J. Physiol.* **432**, 885–892
45. Wightman, R. M., Schroeder, T. J., Finnegan, J. M., Ciolkowski, E. L., and Pihel, K. (1995) Time course of release of catecholamines from individual vesicles during exocytosis at adrenal medullary cells. *Biophys. J.* **68**, 383–390
46. Walker, A., Glavinovic, M. I., and Trifaro, J. M. (1996) Time course of release of content of single vesicles in bovine chromaffin cells. *Plügers Archiv. Euro. J. Physiol.* **431**, 729–735
47. O’Connor, D. T., Klein, R. L., Thureson-Klein, A. K., and Barbosa, J. A. (1991) Chromogranin A: localization and stoichiometry in large dense core catecholamine storage vesicles from sympathetic nerve. *Brain Res.* **567**, 188–196
48. Zhou, Z., Mislser, S., and Chow, R. H. (1996) Rapid fluctuations in transmitter release from single vesicles in bovine adrenal chromaffin cells. *Biophysical J.* **70**, 1543–1552
49. Yamaguchi, M., Yoshitake, T., Fujino, K., Kawano, K., Kehr, J., and Ishida, J. (1999) Determination of norepinephrine in microdialysis samples by microbore column liquid chromatography with fluorescence detection following derivatization with benzylamine. *Anal. Biochem.* **270**, 296–302
50. Castren, E. (2005) Is mood chemistry? Nature reviews. *Neuroscience* **6**, 241–246
51. Schroeder, T. J., Borges, R., Finnegan, J. M., Pihel, K., Amatore, C., and Wightman, R. M. (1996) Temporally resolved, independent stages of individual exocytotic secretion events. *Biophys. J.* **70**, 1061–1068
52. Gong, L. W., Hafez, I., Alvarez de Toledo, G., and Lindau, M. (2003) Secretory vesicles membrane area is regulated in tandem with quantal size in chromaffin cells. *J. Neurosci.* **23**, 7917–7921
53. Colliver, T. L., Pyott, S. J., Achalabun, M., and Ewing, A. G. (2000) VMAT-Mediated changes in quantal size and vesicular volume. *J. Neurosci.* **20**, 5276–5282
54. Jancsar, S. M., Leonard, B. E. (1983) Behavioural and neurochemical interactions between chronic reserpine and

- chronic antidepressants. A possible model for the detection of atypical antidepressants. *Biochem. Pharmacol.* **32**, 1569–1571
55. Nirenberg, M. J., Chan, J., Liu, Y., Edwards, R. H., and Pickel, V. M. (1997) Vesicular monoamine transporter-2: immunogold localization in striatal axons and terminals. *Synapse* **26**, 194–198
56. Chen, B. T., and Rice, M. E. (2001) Novel  $\text{Ca}^{2+}$  dependence and time course of somatodendritic dopamine release: substantia nigra versus striatum. *J. Neurosci.* **21**, 7841–7847
57. Ludwig, M., Bull, P. M., Tobin, V. A., Sabatier, N., Landgraf, R., Dayanithi, G., and Leng, G. (2005) Regulation of activity-dependent dendritic vasopressin release from rat supraoptic neurones. *J. Physiol.* **564**, 515–522
58. Huang, L. Y., Neher, E. (1996)  $\text{Ca}^{2+}$ -dependent exocytosis in the somata of dorsal root ganglion neurons. *Neuron* **17**, 135–145

*Received for publication November 2, 2006.*

*Accepted for publication March 1, 2007.*